LETTER

doi:10.1038/nature11156

Emergence of *KRAS* mutations and acquired resistance to anti-EGFR therapy in colorectal cancer

Sandra Misale[1,2]*, Rona Yaeger[3]*, Sebastijan Hobor[1]*, Elisa Scala[1,2]*, Manickam Janakiraman[4]*, David Liska[5], Emanuele Valtorta[6], Roberta Schiavo[7], Michela Buscarino[1,2], Giulia Siravegna[1], Katia Bencardino[7], Andrea Cercek[3], Chin-Tung Chen[5], Silvio Veronese[6], Carlo Zanon[1], Andrea Sartore-Bianchi[7], Marcello Gambacorta[6], Margherita Gallicchio[8], Efsevia Vakiani[9], Valentina Boscaro[8], Enzo Medico[2,10], Martin Weiser[5], Salvatore Siena[7], Federica Di Nicolantonio[1,11], David Solit[3,4] & Alberto Bardelli[1,2,11]

A main limitation of therapies that selectively target kinase signalling pathways is the emergence of secondary drug resistance. Cetuximab, a monoclonal antibody that binds the extracellular domain of epidermal growth factor receptor (EGFR), is effective in a subset of *KRAS* wild-type metastatic colorectal cancers[1]. After an initial response, secondary resistance invariably ensues, thereby limiting the clinical benefit of this drug[2]. The molecular bases of secondary resistance to cetuximab in colorectal cancer are poorly understood[3–8]. Here we show that molecular alterations (in most instances point mutations) of *KRAS* are causally associated with the onset of acquired resistance to anti-EGFR treatment in colorectal cancers. Expression of mutant *KRAS* under the control of its endogenous gene promoter was sufficient to confer cetuximab resistance, but resistant cells remained sensitive to combinatorial inhibition of EGFR and mitogen-activated protein-kinase kinase (MEK). Analysis of metastases from patients who developed resistance to cetuximab or panitumumab showed the emergence of *KRAS* amplification in one sample and acquisition of secondary *KRAS* mutations in 60% (6 out of 10) of the cases. *KRAS* mutant alleles were detectable in the blood of cetuximab-treated patients as early as 10 months before radiographic documentation of disease progression. In summary, the results identify *KRAS* mutations as frequent drivers of acquired resistance to cetuximab in colorectal cancers, indicate that the emergence of *KRAS* mutant clones can be detected non-invasively months before radiographic progression and suggest early initiation of a MEK inhibitor as a rational strategy for delaying or reversing drug resistance.

Defining the molecular bases of secondary resistance to anti-EGFR therapies is crucial to monitor, prevent and/or overcome drug refractoriness. To identify potential mechanisms of cetuximab resistance, we generated cetuximab-resistant variants of two colorectal cancer (CRC) cellular models (DiFi and Lim1215 cells) that are highly sensitive to EGFR inhibition (Supplementary Fig. 1a). DiFi cells overexpress EGFR as a result of high level amplification of the *EGFR* gene locus[9]. By contrast, Lim1215 cells express 'normal' EGFR levels but are similarly sensitive to cetuximab (Supplementary Fig. 1b, c). Both cell lines are wild type for *KRAS*, *BRAF* and *PIK3CA*, paralleling the molecular features of the patients with CRC who are most likely to respond to cetuximab[10].

Continuous drug treatment using two different protocols (see Methods and Supplementary Fig. 2) led to the emergence of cetuximab-resistant variants (termed DiFi-R and Lim1215-R; Figs 1a and 2a). To identify the molecular basis of cetuximab resistance in these cells, we performed gene copy number analysis and mutational profiling of the resistant and parental lines. Cetuximab-resistant DiFi-R cells differed from their sensitive parental counterpart by two focal molecular alterations: the *EGFR* gene copy number was reduced, whereas the *KRAS* gene was amplified (Fig. 1b, c and Supplementary Fig. 3). These genomic changes were accompanied by reduced EGFR and increased KRAS protein expression in the cetuximab-resistant cells (Fig. 1d). Sequence analysis confirmed that the *EGFR*, *KRAS*, *NRAS*, *HRAS*, *BRAF* and *PIK3CA* genes were all wild type in the cetuximab-resistant clones.

Sequence analysis of the Lim1215 cetuximab-resistant variants identified acquisition of either KRAS(G13D) or KRAS(G12R) mutations (Fig. 2b). In both DiFi-R and Lim1215-R cells, *KRAS* amplification and mutations, respectively, were accompanied by increased KRAS activation relative to their parental counterparts. In the presence of *KRAS* amplification, cetuximab could partially abrogate phosphorylation of MEK and extracellular signal-regulated kinase (ERK) but, as in *KRAS* mutant cells, was unable to induce growth arrest (Figs 1a, d and 2a, c).

To determine whether resistance was due to selection of pre-existing drug-resistant cells, we analysed the parental cell lines in depth for the presence of a minority population of *KRAS* amplified or mutant cells. In the parental DiFi cells, we identified a sub-population with high level *KRAS* amplification at a prevalence of approximately 1:40,000 (Supplementary Fig. 4). Similarly, deep sequencing and BEAMing (bead, emulsion, amplification and magnetics)[11] indicated that approximately 0.2% of the parental Lim1215 cells contained the KRAS(G13D) mutation (Supplementary Table 1). Notably, the G12R mutation was not detectable in the earliest available passage of parental cells, even when the analysis was performed at high coverage (>50,000-fold). These results suggest that the emergence of a cetuximab-resistant population could derive from selection of a pre-existing *KRAS* amplified or mutant clone or as the result of '*de novo*' acquisition of a *KRAS* mutation under the pressure of cetuximab treatment. To assess this latter possibility formally, we performed dilution cloning of the earliest available passage of Lim1215 cells to generate a homogenous, *KRAS* wild-type Lim1215 sub-line. As schematized in Supplementary Fig. 5, two successive dilution cloning experiments were performed and the derivative cells (hereafter referred to as E4.1) were confirmed as *KRAS* wild-type by both mass spectrometry (MS)-based genotyping and 454 pyrosequencing analysis. We then cultured the E4.1 cells in increasing concentrations of cetuximab, analogous to the experiment performed with the original Lim1215 parental line. Cells were collected during intermediate passages and subjected to MS-based genotyping and/or 454 sequencing analysis (Supplementary Fig. 5a).

[1]Laboratory of Molecular Genetics, Institute for Cancer Research and Treatment (IRCC), 10060 Candiolo (Torino), Italy. [2]Department of Oncological Sciences, University of Torino Medical School, 10060 Candiolo (Torino), Italy. [3]Department of Medicine, Memorial Sloan-Kettering Cancer Center, New York, New York 10065, USA. [4]Human Oncology and Pathogenesis Program, Memorial Sloan-Kettering Cancer Center, New York, New York 10065, USA. [5]Department of Surgery, Memorial Sloan-Kettering Cancer Center, New York, New York 10065, USA. [6]Division of Pathology, Ospedale Niguarda Ca' Granda, 20162 Milano, Italy. [7]Falck Division of Medical Oncology, Ospedale Niguarda Ca' Granda, 20162 Milano, Italy. [8]Dipartimento di Scienza e Tecnologia del Farmaco, University of Torino, 10125 Torino, Italy. [9]Department of Pathology, Memorial Sloan-Kettering Cancer Center, New York, New York 10065, USA. [10]Laboratory of Functional Genomics, Institute for Cancer Research and Treatment (IRCC), 10060 Candiolo (Torino), Italy. [11]FIRC Institute of Molecular Oncology (IFOM), 20139 Milano, Italy.
*These authors contributed equally to this work.

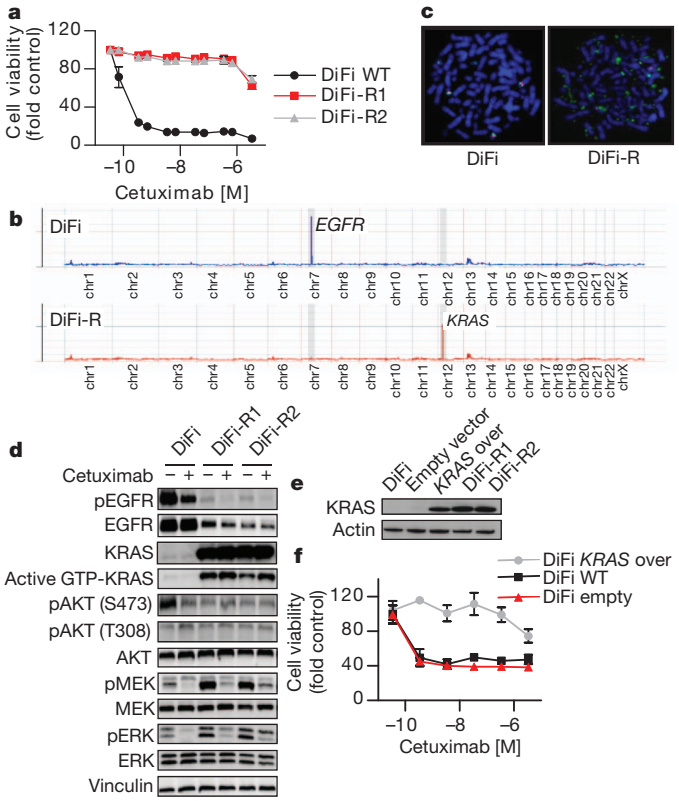

Figure 1 | *KRAS* amplification mediates acquired resistance to cetuximab in DiFi cells. **a**, Parental (wild-type, WT) and cetuximab-resistant (-R1, -R2) DiFi cells were treated for one week with increasing concentrations of cetuximab. Cell viability was assayed by the ATP assay. Data points represent the mean ± s.d. of three independent experiments. **b**, Whole exome gene copy number analysis of parental and cetuximab-resistant DiFi cells. Individual chromosomes are indicated on the *x*-axis. The lines indicate the sequencing depth (*y*-axis) over exome windows of 100,000 base pairs. **c**, Fluorescent *in situ* hybridization (FISH) analysis confirming *KRAS* amplification in resistant (DiFi-R) but not parental DiFi cells. *KRAS* locus bacterial artificial chromosome (BAC) DNA (probe RP11-707G18; green) and chromosome 12 paint (red) were hybridized to the metaphase spreads of DiFi cells. Original magnification, ×100. **d**, DiFi cells were treated with 35 nM cetuximab for 24 h, and whole-cell extracts were then subjected to western blot analysis and compared with untreated cells. DiFi-R1 and -R2 cells were plated in the absence of cetuximab for 7 days or maintained in their normal growth medium (with 35 nM cetuximab) before protein analysis. Active KRAS (GTP-KRAS) was assessed by glutathione *S*-transferase (GST)–RAF1 pull-down. Whole-cell extracts were blotted with phosphorylated EGFR (pEGFR; Tyr 1068), total EGFR, total KRAS, phosphorylated AKT (Thr 308), phosphorylated AKT (Ser 473), total AKT, total MEK1/2 and phosphorylated MEK1/2, total ERK1/2 and phosphorylated ERK1/2 antibodies. Vinculin was included as a loading control. **e**, Western blot analysis of KRAS protein in DiFi cells infected with a *KRAS* lentivirus. Actin is shown as a loading control. **f**, Ectopic expression of wild-type *KRAS* in parental DiFi cells confers resistance to cetuximab. Data points represent the mean ± s.d. of three independent experiments.

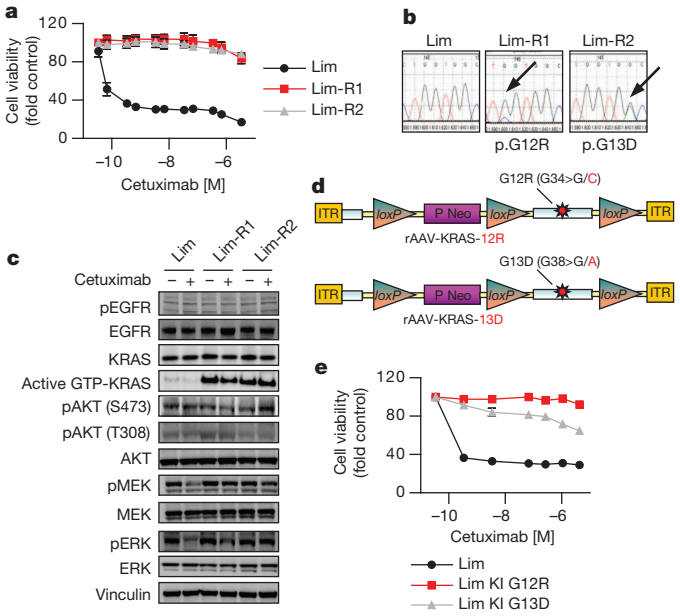

Figure 2 | *KRAS* mutations mediate acquired resistance to cetuximab in Lim1215 cells. **a**, Parental (Lim) and cetuximab-resistant (Lim-R1 and Lim-R2) Lim1215 cells were treated for one week with increasing concentrations of cetuximab. Cell viability was assayed by the ATP assay. Data points represent the mean ± s.d. of three independent experiments. **b**, Sanger sequencing of *KRAS* exon 2 in parental and two representative cetuximab-resistant Lim1215 cells obtained in independent selection procedures. **c**, Western blot analysis of the EGFR signalling pathway in parental and cetuximab-resistant Lim1215 cells. **d**, Schematic representation of the vectors used to knock-in the G12R and G13D mutations into the genome of Lim1215 parental cell lines by AAV-mediated homologous recombination. Targeting was assessed by Sanger sequencing. ITR, inverted terminal repeat; P Neo, neomycin-resistance plasmid. **e**, Parental and isogenic Lim1215 cells carrying the indicated mutations were treated for one week with increasing doses of cetuximab. KI, knock-in. Data points represent the mean ± s.d. of three independent experiments.

MS genotyping identified a KRAS(A146T) mutation after four passages in increasing concentrations of cetuximab (20 nM and higher; Supplementary Fig. 5b). These cells were indeed resistant to the drug (Supplementary Fig. 5c, d), and showed biochemical activation of KRAS (Supplementary Fig. 5e). In parallel, genetic analysis of the E4.1 cells grown in medium without cetuximab found them to be *KRAS* wild type. In summary, these data suggest that resistance to cetuximab in Lim1215 cells may emerge not only from the selection of pre-existing *KRAS* mutant clones but also as a result of continuing mutagenesis.

To prove that amplification or mutations of *KRAS* were causally responsible for cetuximab resistance in our *in vitro* models, we performed two sets of forward genetic experiments. First, ectopic overexpression of wild-type *KRAS* in DiFi conferred resistance to cetuximab (Fig. 1e, f). Second, adeno-associated virus (AAV)-mediated targeted homologous recombination was used to introduce (knock-in) the G13D and G12R alleles into the endogenous *KRAS* locus of Lim1215 cells[12]. Knock-in of the G13D or G12R mutant alleles rendered Lim1215 cells resistant to cetuximab (Fig. 2d, e).

Patients with chemotherapy-refractory CRC, who initially respond and then become resistant to cetuximab, have no further therapeutic options. We reasoned that cetuximab resistance resulting from constitutive KRAS activation could be prevented or reversed by pharmacological inhibition of KRAS signalling. We thus co-treated the resistant clones with cetuximab and selective inhibitors of MEK kinase and phosphatidylinositol-3-OH kinase (PI(3)K)—two key downstream effectors of oncogenic KRAS. Although PI(3)K inhibitors were ineffective in the cetuximab-resistant cells, both the Lim1215-R and DiFi-R cells were sensitive to combinatorial targeting of MEK and EGFR (Supplementary Fig. 6).

To determine whether *KRAS* mutation and/or amplification are clinically relevant mechanisms of acquired cetuximab resistance, we examined tumour biopsies from ten patients with CRC who had become refractory to either cetuximab or the anti-EGFR antibody panitumumab (Supplementary Table 2). We identified one individual (patient 11, Supplementary Table 3a) whose tumour at progression displayed *KRAS* amplification that was not present in a matched pre-cetuximab biopsy (Supplementary Fig. 7). In a different patient (patient 8, Supplementary Table 3a) Sanger sequencing identified a KRAS(Q61H) mutation in a biopsy obtained after disease progression on cetuximab treatment; the remaining eight tumour samples

obtained in patients with acquired resistance to anti-EGFR therapy were wild-type *KRAS* by this technique (Supplementary Table 3a). To determine whether the Sanger technology may have been underpowered to detect *KRAS* mutations in the biopsies obtained after cetuximab or panitumumab progression, these remaining cases were analysed using either 454 deep sequencing or BEAMing. These techniques identified the KRAS(G13D) mutation in four samples, and the simultaneous presence of G12D and G13D mutations in one case (Fig. 3b). In the six patients for whom sufficient pre-treatment tumour samples were available for high coverage 454 sequence analysis or BEAMing, *KRAS* mutations were absent pre-treatment (Supplementary Table 3b). Tumours from a further eight patients treated with cytotoxic chemotherapy but not previously exposed to anti-EGFR therapies were also analysed by 454 deep sequencing. In all eight cases (patients 13–21), 454 sequence analyses identified no evidence of *KRAS* mutation (Fig. 3a). These results indicate that treatment with anti-EGFR antibodies but not cytotoxic chemotherapy is associated with the acquisition of *KRAS* mutations ($P = 0.0193$) (Fig. 3c). Our data support the initiation of clinical trials to define the prevalence of *KRAS* alterations as a mechanism of acquired resistance to anti-EGFR therapies through systematic collection of biopsies.

Emergence of secondary resistance to cetuximab (disease progression) is presently established by radiological evaluation, and typically occurs within 9 to 18 months. We reasoned that the detection of *KRAS* mutant alleles in the plasma of patients treated with cetuximab or panitumumab may allow the early identification of individuals at risk for this mechanism of drug resistance before radiographic documentation of disease progression. We thus performed BEAMing analysis of serial plasma samples from patients treated with cetuximab (Supplementary Table 4a, b). This analysis confirmed that the same *KRAS* variants that were ultimately identified in the post-treatment (disease progression) biopsies were detectable in plasma as early as 10 months before the documentation of disease progression by radiological assessment (Fig. 4).

Drugs that target activated kinase pathways have profound but often temporary anti-tumour effects in subsets of patients with advanced solid tumours. In patients with advanced CRC, antibodies that bind to the extracellular domain of EGFR induce tumour regressions in 10–15% of patients when used alone, and enhance the effects of cytotoxic chemotherapies when used in combination[13,14]. Although several previous studies have identified somatic mutations in the *KRAS* gene as a biomarker of intrinsic resistance to EGFR-targeted agents in patients with CRC[2,15], the molecular basis for acquired resistance has remained obscure. We now report, for the first time, that a substantial fraction of CRC patients who exhibit an initial response to anti-EGFR therapies have, at the time of disease progression, tumours with focal amplification or somatic mutations in *KRAS* that were not detectable before the initiation of therapy. Our data indicate that drug resistance resulting from alterations in *KRAS* can be attributed not only to the selection of pre-existent *KRAS* mutant and amplified clones, but also to new mutations that arise as the result of continuing mutagenesis. The percentage of *KRAS* mutant alleles detected in the resistant tumours ranged from 0.4 to 17% (Fig. 3). At least three (not mutually exclusive) possibilities could account for this low allele frequency. First, despite our efforts to maximize tumour content by macrodissecting each sample, the individual tumour biopsies consisted of variable proportions of tumour and intermixed wild-type *KRAS* stromal cells. Second, only a fraction of the tumour cells in the disease progression samples may have contained the 'resistance' mutation. The latter model has been observed in patients with lung cancer with secondary resistance to the EGFR inhibitor erlotinib, in which only a fraction of the tumour cells collected at the time of radiographic disease progression contain

a

	Chemotherapy-resistant tumours *KRAS* mutational status		
Patient ID	Mutation	Percentage	Reads*/events†
2	WT*	0%	0/30,000
7	WT*	0%	0/11,262
8	WT†	0.01%	5/76,200
9	WT†	0%	0/89,760
10	WT†	0%	0/34,500
11	WT†	0%	0/190,600
13	WT*	0%	0/18,277
14	WT*	0%	0/27,942
15	WT*	0%	0/43,279
16	WT*	0%	0/41,693
17	WT*	0%	0/30,174
18	WT*	0%	0/16,400
19	WT*	0%	0/29,578
21	WT*	0%	0/18,277

b

	Anti-EGFR-resistant tumours *KRAS* mutational status		
Patient ID	Mutation	Percentage	Reads*/events†
1	WT*	0%	0/12,123
2	G13D*	10%	859/8,556
4	G13D*	5.9%	461/7,764
5	G13D*	14.3%	1,037/7,247
6	G13D*	8.6%	651/7,577
7	WT*	0%	0/17,142
8	Q61H†	17.3%	5,960/190,200
9	G12D† G13D†	0.04% 0.44%	17/40,200 117/26,400
10	WT†	0%	0/50,300
11	WT† (KRAS amplified)	0%	0/30,400

c

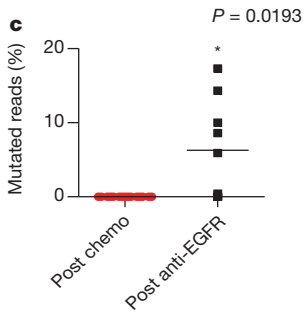

Figure 3 | Mutational analysis of the *KRAS* gene in patients. **a**, Mutational analysis of *KRAS* in patients with chemotherapy-refractory CRC. **b**, Mutational analysis of the *KRAS* gene in patients who progressed on anti-EGFR antibodies. The results in **a** and **b** are based on assays performed by deep sequencing technologies, either 454 pyrosequencing (*) or BEAMing (†). **c**, Dot plot of the percentage of mutated *KRAS* alleles in patients with chemotherapy-refractory and anti-EGFR-resistant CRC. *P* value was calculated using a two-tailed unpaired Mann–Whitney test.

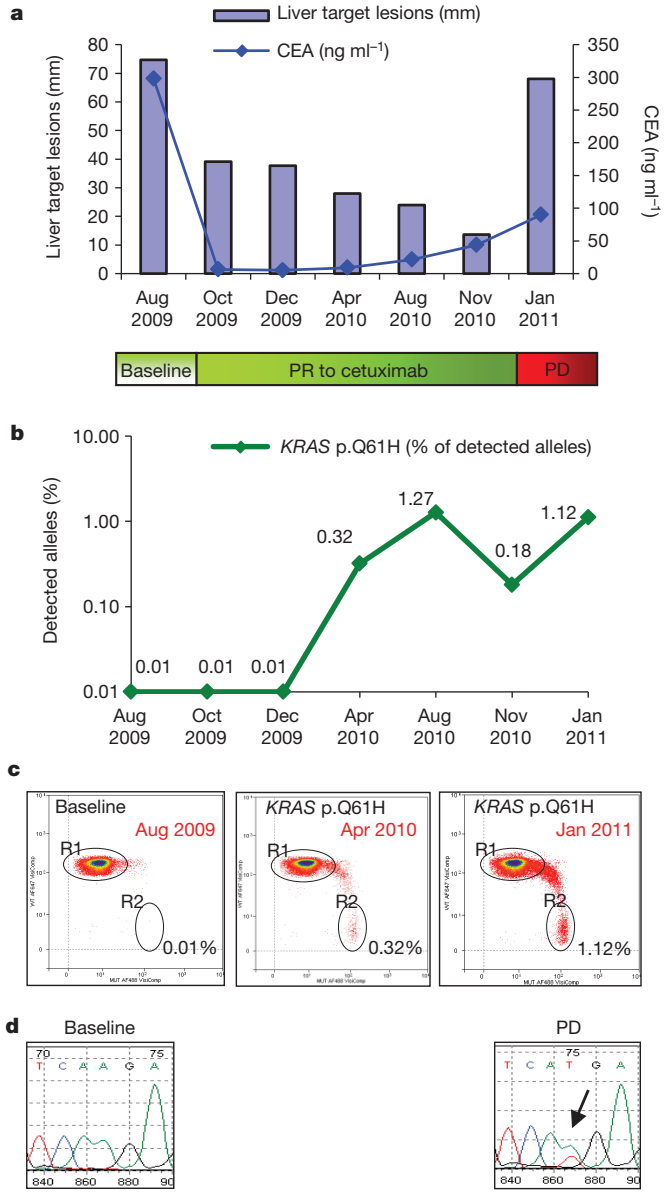

Figure 4 | Detection of circulating *KRAS* mutant DNA in a patient with acquired resistance to cetuximab therapy. **a**, Size of liver metastasis (blue bars) and carcinoembryonic antigen (CEA) levels in blood (blue line) at the indicated time points, showing an initial response to cetuximab followed by progression (patient 8). PR, partial response; PD, progressive disease. **b**, Quantitative analysis of KRAS(Q61H) mutant DNA in plasma, as assessed by BEAMing. **c**, Two-dimensional dot plot showing quantitative analysis of the KRAS(Q61H) mutation in plasma using BEAMing at individual time points. **d**, Mutational analysis of *KRAS* on tumour samples collected before cetuximab treatment and at the time of disease progression.

the EGFR(T790M) 'resistant' allele[16–18]. Analogously, a recent study indicates that a subset of colorectal cancers found to be wild-type *KRAS* by conventional Sanger sequencing, but *KRAS* mutant by more sensitive techniques, do not respond to anti-EGFR treatment[19]. These data suggest that clinical drug resistance may result from the acquisition of a drug-resistant allele in a sub-population of tumour cells. Finally, it is plausible that independent cell populations containing different resistance mechanisms evolve in parallel within the same metastatic lesion. Nevertheless, our functional analyses in cell models show that *KRAS* mutations are causally responsible for acquired resistance to cetuximab.

Furthermore, we find that the *KRAS* mutant alleles found in the tumours of patients collected after radiographic disease progression can be detected in plasma using highly sensitive DNA analysis methods. As such tumours may be sensitive to combined treatment with a MEK inhibitor, our results suggest that blood-based non-invasive monitoring of patients undergoing treatment with anti-EGFR therapies for the emergence of *KRAS* mutant clones could allow for the early initiation of combination therapies that may delay or prevent disease progression.

METHODS SUMMARY

DiFi and Lim1215 cells were exposed to different doses of cetuximab as described in Supplementary Fig. 2 to obtain the resistant variants. Cell viability was assessed by ATP content. Cells were seeded in 100 µl medium in 96-well plastic culture plates. The experimental procedures for knock-in of cancer mutations, the vectors, AAV production, cell infection and screening for recombinants have been described elsewhere[12]. Tumour specimens were obtained through protocols approved by the Institutional Review Board of Memorial Sloan-Kettering Cancer Center (protocol 10-029) and Ospedale Niguarda Ca' Granda (protocols 1014/09 and 194/2010). Details about the clinical characteristics of patients are provided in Supplementary Table 2. Identification of cancer mutations in the *KRAS*, *HRAS*, *NRAS*, *BRAF*, *PIK3CA* and *EGFR* genes was performed with different sequencing platforms (Sanger, 454 pyrosequencing and mass spectrometry), as described in detail in the Methods. For immunoblot analysis, total cellular proteins were extracted by solubilizing the cells in boiling SDS buffer. Western blot detection was done by enhanced chemiluminescence. The analysis of KRAS activation was performed by immunoprecipitation assay with a glutathione *S*-transferase (GST) fusion protein containing the Ras-binding domain (RBD) of RAF1 (GST–RAF1-RBD). Real-time PCR was performed using an ABI PRISM 7900HT apparatus (Applied Biosytems). KRAS protein expression was evaluated by immunohistochemistry performed on 3-µm-thick tissue sections using a specific KRAS (F234) antibody (SC-30, mouse monoclonal IgG_{2a} Santa Cruz Biotechnology). BEAMing was performed essentially as described previously[10], with deviations from the original protocol outlined in Methods. FISH experiments were conducted with the histology FISH accessory kit (Dako). Data are presented as mean ± s.d. and $n = 3$. Statistical significance was determined by a paired Student's *t*-test or unpaired Mann–Whitney test. $P < 0.05$ was considered statistically significant.

Full Methods and any associated references are available in the online version of the paper at www.nature.com/nature.

Received 8 December 2011; accepted 23 April 2012.
Published online 13 June 2012.

1. Ciardiello, F. & Tortora, G. EGFR antagonists in cancer treatment. *N. Engl. J. Med.* **358,** 1160–1174 (2008).
2. Karapetis, C. S. *et al. K-ras* mutations and benefit from cetuximab in advanced colorectal cancer. *N. Engl. J. Med.* **359,** 1757–1765 (2008).
3. Wheeler, D. L. *et al.* Mechanisms of acquired resistance to cetuximab: role of HER (ErbB) family members. *Oncogene* **27,** 3944–3956 (2008).
4. Benavente, S. *et al.* Establishment and characterization of a model of acquired resistance to epidermal growth factor receptor targeting agents in human cancer cells. *Clin. Cancer Res.* **15,** 1585–1592 (2009).
5. Li, C., Iida, M., Dunn, E. F., Ghia, A. J. & Wheeler, D. L. Nuclear EGFR contributes to acquired resistance to cetuximab. *Oncogene* **28,** 3801–3813 (2009).
6. Hatakeyama, H. *et al.* Regulation of heparin-binding EGF-like growth factor by miR-212 and acquired cetuximab-resistance in head and neck squamous cell carcinoma. *PLoS ONE* **5,** e12702 (2010).
7. Yonesaka, K. *et al.* Activation of ERBB2 signaling causes resistance to the EGFR-directed therapeutic antibody cetuximab. *Sci. Transl. Med.* **3,** 99ra86 (2011).
8. Montagut, C. *et al.* Identification of a mutation in the extracellular domain of the Epidermal Growth Factor Receptor conferring cetuximab resistance in colorectal cancer. *Nature Med.* **18,** 221–223 (2012).
9. Moroni, M. *et al.* Gene copy number for epidermal growth factor receptor (EGFR) and clinical response to antiEGFR treatment in colorectal cancer: a cohort study. *Lancet Oncol.* **6,** 279–286 (2005).
10. De Roock, W. *et al.* Effects of *KRAS*, *BRAF*, *NRAS*, and *PIK3CA* mutations on the efficacy of cetuximab plus chemotherapy in chemotherapy-refractory metastatic colorectal cancer: a retrospective consortium analysis. *Lancet Oncol.* **11,** 753–762 (2010).
11. Diehl, F. *et al.* Circulating mutant DNA to assess tumor dynamics. *Nature Med.* **14,** 985–990 (2008).
12. Di Nicolantonio, F. *et al.* Replacement of normal with mutant alleles in the genome of normal human cells unveils mutation-specific drug responses. *Proc. Natl Acad. Sci. USA* **105,** 20864–20869 (2008).
13. Bardelli, A. & Siena, S. Molecular mechanisms of resistance to cetuximab and panitumumab in colorectal cancer. *J. Clin. Oncol.* **28,** 1254–1261 (2010).
14. Van Cutsem, E. *et al.* Cetuximab and chemotherapy as initial treatment for metastatic colorectal cancer. *N. Engl. J. Med.* **360,** 1408–1417 (2009).

15. Amado, R. G. *et al.* Wild-type KRAS is required for panitumumab efficacy in patients with metastatic colorectal cancer. *J. Clin. Oncol.* **26,** 1626–1634 (2008).
16. Janne, P. A. Challenges of detecting EGFR T790M in gefitinib/erlotinib-resistant tumours. *Lung Cancer* **60** (suppl. 2), S3–S9 (2008).
17. Engelman, J. A. *et al.* Allelic dilution obscures detection of a biologically significant resistance mutation in EGFR-amplified lung cancer. *J. Clin. Invest.* **116,** 2695–2706 (2006).
18. Arcila, M. E. *et al.* Rebiopsy of lung cancer patients with acquired resistance to EGFR inhibitors and enhanced detection of the T790M mutation using a locked nucleic acid-based assay. *Clin. Cancer Res.* **17,** 1169–1180 (2011).
19. Molinari, F. *et al.* Increased detection sensitivity for *KRAS* mutations enhances the prediction of anti-EGFR monoclonal antibody resistance in metastatic colorectal cancer. *Clin. Cancer Res.* **17,** 4901–4914 (2011).

Supplementary Information is linked to the online version of the paper at www.nature.com/nature.

Acknowledgements We are particularly indebted to S. Lamba for generating the KRAS(G12R) knock-in in Lim1215 cells. We thank C. Cancelliere and S. Destefanis for technical assistance. We thank S. Arena, M. Russo and D. Zecchin for critically reading the manuscript. We also thank A. Heguy, A. Viale, N. Socci and M. Pirun for assistance with analysis of next generation sequencing data. This work was supported by European Union Seventh Framework Programme, grant 259015 COLTHERES (A.B. and S.S.); Associazione Italiana per la Ricerca sul Cancro (AIRC) 2010 Special Program Molecular Clinical Oncology 5 × 1000, project 9970 (A.B. and S.S.); Regione Piemonte (A.B. and F.D.N.); Fondazione Piemontese per la Ricerca sul Cancro (FPRC) Intramural Grant, 5xmille 2008, ONLUS (A.B. and F.D.N.); AIRC MFAG 11349 (F.D.N.); Oncologia Ca' Granda ONLUS (OCGO) (S.S.); Mr William H. Goodwin and Mrs Alice Goodwin and the Commonwealth Foundation for Cancer Research; the Experimental Therapeutics Center of Memorial Sloan-Kettering Cancer Center (D.S.); the Society of MSKCC (M.W.); the National Institutes of Health (D.S.); the Beene Foundation (D.S.) and Regione Lombardia and Ministerio Salute grant 'Gene Mutation Monitoring in mCRC' (S.S.).

Author Contributions A.B., D.S., S.S. and F.D.N. planned the project and supervised all research. A.B., D.S. and F.D.N. wrote the manuscript. S.M., R.Y., S.H., E.S., M.W. and F.D.N. designed the experiments. A.B. conceived the molecular analysis of plasma samples. S.M., R.Y., S.H., E.S., M.J., D.L., E.V., R.S., M.B., G.S., C.-T.C., S.V., M.G. and V.B. performed the experiments. C.Z., A.S.-B., M.G. and E.M. analysed data. K.B., A.C. and E.V. provided samples for analysis. S.S., D.S. and A.B. devised dual biopsy clinical protocols for EGFR mAb resistant mCRC.

Author Information Reprints and permissions information is available at www.nature.com/reprints. The authors declare no competing financial interests. Readers are welcome to comment on the online version of this article at www.nature.com/nature. Correspondence and requests for materials should be addressed to D.S. (solitd@mskcc.org) or A.B. (alberto.bardelli@ircc.it).

METHODS

Cell culture and generation of resistant cells. DiFi cells were cultured in F12 medium (Invitrogen) supplemented with 5% FBS, and Lim1215 cells were cultured in RPMI-1640 medium (Invitrogen) supplemented with 5% FBS and 1 μg ml^{-1} insulin. DiFi parental cells were plated in 100 mm Petri dishes with 2.5% FBS, and exposed to a constant dose of cetuximab (350 nM) for one year to obtain the resistant counterpart DiFi-R1. The DiFi-R2 derivative was obtained by increasing the cetuximab dosage stepwise from 3.5 nM to 350 nM during the course of a year. The same protocols were applied to Lim1215 cells, with variations with respect to cetuximab concentrations: for Lim-R1, cetuximab was used at 1,400 nM, and for Lim-R2, the drug concentration increased stepwise from 350 nM to 1,400 nM. For Lim1215, both protocols required at least 3 months of drug treatment. The Lim1215 parental cell line had been described previously[20] and was obtained from R. Whitehead, with permission from the Ludwig Institute for Cancer Research. The genetic identity of the cell lines used in this study was confirmed by short tandem repeat (STR) profiling (Cell ID, Promega)

Drug viability assays. Cetuximab was obtained from Pharmacy at Niguarda Ca' Granda Hospital. The MEK inhibitor AZD6244 and the PI(3)K inhibitor GSK1059615 were purchased from Sequoia Chemicals and Selleck Chemicals, respectively. Cell lines were seeded in 100 μl medium at appropriate densities (5×10^4 and 1.5×10^4 cells per well for DiFi and Lim1215 cells, respectively) in 96-well plastic culture plates. After serial dilutions, drugs in serum-free medium were added to cells, and medium-only containing wells were added as controls. Plates were incubated at 37 °C in 5% CO_2 for 72–168 h, after which cell viability was assessed by ATP content using the CellTiter-Glo luminescent assay (Promega).

Mutational analysis. RAS genotyping was performed using the iPLEX assay (Sequenom), which is based on a single-base primer extension assay. In brief, multiplexed PCR and extension primers are designed for a panel of known mutations. After PCR and extension reactions, the resulting extension products are analysed using a matrix-assisted laser desorption/ionization–time-of-flight (MALDI–TOF) mass spectrometer. For 454 picotiter plate pyrosequencing (Roche), PCR products were generated using primers designed to span exons 2, 3 and 4 in *KRAS* and adapted with 5′ overhangs to facilitate emulsion PCR (emPCR) and sequencing. After amplification by emPCR, beads containing DNA were isolated. A total of 34,000 beads were sequenced in both directions, yielding 1,000–5,000 sequencing reads on average per sample (~1,000 reads per amplicon per sample) using GSFLX. To detect variants in 454 pyrosequencing data, reads were mapped with the Burrows-Wheeler aligner (BWA) using the bwasw mode for aligning long reads. The generated SAM file was then run through the Picard MarkDuplicate program to remove duplicated reads (reads with the same initial starting point). The file was then processed with the GATK BaseQ recalibrator. Finally, we generated pileups using Samtools and called variants using VarScan. For Sanger sequencing, all samples were subjected to automated sequencing by ABI PRISM 3730 (Applied Biosystems). All mutations were confirmed twice, starting from independent PCR reactions.

All primer sequences are available on request. Exome sequencing was carried out by exome capture using the SeqCap EZ human exome library v1.0 (Nimblegen) and subsequent pyrosequencing of the captured fragments by means of 454Flx sequencer (Roche), according to the manufacturer's protocols. A total of 1.2 million reads were sequenced for an average exome depth of ×4. The reads were mapped using the manufacturer's mapping tools and the depth of the reads was used as an estimator of the copy number value in the two parental and resistant DiFi samples. Average read depths were calculated within overlapping 100,000-base-pair wide windows for Fig. 1b, whereas average read depths were calculated for exons and genes and plotted as dots and segments, respectively, in Supplementary Fig. 3a, b.

Tissue procurement. Tumour specimens were obtained through protocols approved by the Institutional Review Board of Memorial Sloan-Kettering Cancer Center (protocol 10-029) and Ospedale Niguarda Ca' Granda (protocols 1014/09 and 194/2010). All tumour specimens were formalin-fixed paraffin-embedded. All patients provided informed consent and samples were procured and the study was conducted under the approval of the Review Boards and Ethical Committees of the Institutions. Details about the clinical characteristic of the patients are provided in Supplementary Table 2.

BEAMing procedure. DNA was extracted from plasma using the QIAamp circulating nucleic acid kit (QIAGEN) according to manufacturer's instructions. BEAMing was performed as described previously[11]. The first amplification was performed in a 50 μl PCR reaction, containing DNA isolated from 1 ml of plasma, 1× Phusion high-fidelity buffer, 1.5 U Hotstart Phusion polymerase (NEB, BioLabs), 0.5 μM of each primer with tag sequence, 0.2 mM of each deoxynucleoside triphosphate, and 0.5 mM $MgCl_2$. Amplification was carried out using the following cycling conditions: 98 °C for 45 s; 2 cycles of 98 °C for 10 s, 67 °C for 10 s, 72 °C for 10 s; 2 cycles of 98 °C for 10 s, 64 °C for 10 s, 72 °C for 10 s; 2 cycles of 98 °C for 10 s, 61 °C for 10 s, 72 °C for 10 s; 31 cycles of 98 °C for 10 s, 58 °C for 10 s, 72 °C for 10 s. PCR products were diluted, and quantified using the PicoGreen double-stranded DNA assay (Invitrogen). A clonal bead population is generated performing emPCR. PCR mixture (150 μl) was prepared containing 18 pg template DNA, 40 U platinum Taq DNA polymerase (Invitrogen), 1× platinum buffer, 0.2 mM dNTPs, 5 mM $MgCl_2$, 0.05 μM Tag1 (TCCCGCGAAATTAATACGAC), 8 μM Tag2 (GCTGGAGCTCTGCAGCTA) and 6×10^7 magnetic streptavidin beads (MyOne, Invitrogen) coated with Tag1 oligonucleotide (dual biotin-TSpacer18-TCCCGCGAAATTAATACGAC). The 150-μl PCR reactions were distributed into the wells of a 96-well PCR plate together with 70 μl of the emusifire oil. The water-in-oil emulsion was obtained by pipetting. The PCR cycling conditions were: 94 °C for 2 min; 50 cycles of 94 °C for 10 s, 58 °C for 15 s, 70 °C for 15 s. All primer sequences are available on request.

Immunoblot analysis. Before biochemical analysis, all cells were grown in their specific media supplemented with 5% FBS. Total cellular proteins were extracted by solubilizing the cells in boiling SDS buffer (50 mM Tris-HCl, pH 7.5, 150 mM NaCl and 1% SDS). Western blot detection was done by enhanced chemiluminescence (GE Healthcare). The following antibodies were used for western blotting (all from Cell Signaling Technology, except where indicated): anti-phospho-AKT S473; anti-phospho-AKT T308; anti-AKT; anti-phospho-p44/42 ERK (Thr 202/Tyr 204); anti-p44/42 ERK; anti-P-MEK1/2 (Ser 217/221), anti-MEK1/2; anti-KRAS (Santa Cruz); anti-EGFR (clone13G8, Enzo Life Sciences); anti-phospho EGFR (Tyr 1068); anti-actin and anti-vinculin (Sigma-Aldrich).

KRAS activation assay (RAS-GTP). The analysis of KRAS activation was performed by an immunoprecipitation assay with a GST fusion protein containing the Ras-binding domain (RBD) of RAF1 (GST–RAF1-RBD), as previously described[12]. The KRAS protein was detected with an anti-KRAS (F234) monoclonal antibody (Santa Cruz).

Gene copy number analysis. Parental and resistant cell lines were trypsinized, washed with PBS and centrifuged; pellets were lysed and DNA was extracted using the wizard SV genomic kit (Promega) according to the manufacturer's directions. Real-time PCR was performed with 150 ng of DNA per single reaction using GoTaq QPCR Master Mix (Promega) and determined by real-time PCR using an ABI PRISM 7900HT apparatus (Applied Biosytems).

All primer sequences are available on request. Exome sequencing was carried out by exome capture using the SeqCap EZ Human Exome Library v1.0 (Nimblegen) and subsequent pyrosequencing of the captured fragments by means of 454Flx sequencer (Roche), according to manufacturer's protocols. A total of 1.2 million reads were sequenced for an average exome depth of ×4. The reads were mapped using the manufacturer's mapping tools and the depth of the reads was determined and used as an estimator of the copy number value in the two parental and resistant DiFi samples. Average read depths within overlapping 100,000-base-pair wide windows were calculated and plotted in Fig. 1c; average read depths within exons and genes were calculated and plotted as dots and segments, respectively, in Supplementary Fig. 4a, b.

Immunohistochemistry assay. KRAS protein expression was evaluated by immunohistochemistry performed on 3-μm-thick tissue sections using a specific KRAS (F234) antibody (SC-30, mouse monoclonal IgG_{2a} Santa Cruz Biotechnology; dilution 1:100) and the automated system BenchMark Ultra (Ventana Medical System, Roche) according to the manufacturers' instructions, with minimum modifications. KRAS protein expression was detected at the cytoplasmatic and membrane level. Samples were considered positive when the expression of protein was present in at least 10% of cells. Healthy tissue, that is, normal colon mucosa, was used as an internal negative control; a slide with the DiFi-R2 cell line was used as an external positive control. Images were captured with the AxiovisionLe software (Zeiss) using an Axio Zeiss Imager 2 microscope (Zeiss).

FISH analysis. All analyses were performed on 3-μm-thick sections of formalin-fixed paraffin-embedded tumour tissue, provided by the Department of Anatomy Pathology of Niguarda Hospital, and on metaphase chromosomes and interphase nuclei, obtained from the DiFi cell line culture following the standard procedures. Tissue sections for FISH experiment were prepared according to the manufacturer's instructions of the histology FISH accessory kit (Dako). For both types of sample the last steps before hybridization were: dehydration in ethanol series (70%, 90% and 100%), three washes (5 min each) and air drying.

Dual colour FISH analysis was performed using a 10-μl mix-probe made up by 1 μl CEP12 α-satellite probe (12p11-q11) labelled in SpectrumOrange (Vysis), 1 μl BAC genomic probe RP11-707G18 (12p12.1) spanning an approximately 176-kilobase region encompassing the *KRAS* gene, labelled in SpectrumGreen (Bluegnome[21]) and 8 μl LSI-WCP hybridization buffer (Vysis) for each slide. Probes and target DNA of specimens were co-denatured in HYBRite System (Dako) for 5 min at 75 °C and then hybridized overnight at 37 °C. Slides were washed with post-hybridization buffer (Dako) at 73 °C for 2 min and counterstained with 4′,6-diamidino-2-phenylindole (DAPI II; Vysis). FISH signals were evaluated with a Zeiss Axioscope Imager.Z1 (Zeiss) equipped with

single and triple band pass filters. Images for documentation were captured with CCD camera and processed using the MetaSystems Isis software. Samples with a ratio greater than 3 between *KRAS* gene and chromosome 12 centromere signals, in at least 10% of 100 cells analysed in 10 different fields, were scored as positive for *KRAS* gene amplification. Healthy tissue, that is, normal colon mucosa, was used as an internal negative control.

Plasmids and viral vectors. All experimental procedures for targeting vector construction, AAV production, cell infection and screening for recombinants have been described elsewhere[12].

Statistical analysis. Data are presented as the mean ± s.d. and $n = 3$. Statistical significance was determined by a paired Student's *t*-test or two-tailed unpaired Mann–Whitney test (Fig. 3c). $P < 0.05$ was considered statistically significant.

20. Whitehead, R. H., Macrae, F. A., St John, D. J. & Ma, J. A colon cancer cell line (LIM1215) derived from a patient with inherited nonpolyposis colorectal cancer. *J. Natl. Cancer Inst.* **74,** 759–765 (1985).
21. Smith, G. *et al.* Activating K-Ras mutations outwith 'hotspot' codons in sporadic colorectal tumours - implications for personalised cancer medicine. *Br. J. Cancer* **102,** 693–703 (2010).